

Plant-mediated synthesis of silver-nanocomposite as novel effective azo dye adsorbent

Mantosh Kumar Satapathy · Priya Banerjee ·
Papita Das

Received: 21 October 2013 / Accepted: 9 December 2013 / Published online: 25 December 2013
© The Author(s) 2013. This article is published with open access at Springerlink.com

Abstract Toxicity of textile effluent is a globally alarming issue nowadays. In order to address this problem, a cost-effective and environment-friendly technique for adsorption of toxic dyes has been introduced in this research. Firstly in this study, green synthesis of silver nanoparticles (AgNPs) having antibacterial efficacy, had been carried out using leaf extracts of *Azadirachta indica* as reducing as well as capping agent. This research idea was further extended for the development and application of a novel method of preparation of silver-nanocomposite using synthesized microwave-assisted AgNPs with soil as a novel nanocomposite to adsorb hazardous dyes. However, this nanocomposite was found to possess higher efficiency and adsorption capacity in comparison to soil as adsorbent for the removal of crystal violet dye under same experimental conditions. Additionally, it was also observed that use of this Ag-nanocomposite as adsorbent helped in achieving about 97.2 % removal of crystal violet dye from the effluent solution.

Keywords Ag-nanoparticle · Nanocomposite · Crystal violet · Dye reduction · *Azadirachta indica*

List of symbols

A	Arrhenius constant
C_a	Equilibrium dye concentration on the nanocomposite (mg L^{-1})
C_e	Equilibrium dye concentration in solution (mg L^{-1})
C_i	Initial dye concentration (mg L^{-1})
E	Mean free energy (kJ mol^{-1})
E_a	Activation energy (kJ mol^{-1})
ΔG^0	Gibbs free energy change (kJ mol^{-1})
ΔH^0	Enthalpy of reaction (kJ mol^{-1})
h	Initial adsorption rate ($\text{mg g}^{-1} \text{min}^{-1}$)
I	Intraparticle diffusion model constant
K_C	Distribution coefficient for adsorption
K_F	Freundlich constant (mg g^{-1}) (L g^{-1}) ^{1/n}
K_L	Langmuir constant (L mg^{-1})
k	Rate constant
k_i	Intraparticle diffusion rate constant ($\text{mg g}^{-1} \text{min}^{-0.5}$)
k_1	Pseudo-first-order rate constant (min^{-1})
k_2	Pseudo-second-order rate constant ($\text{g mg}^{-1} \text{min}^{-1}$)
m	Mass of nanocomposite (g)
n	Freundlich adsorption isotherm constant
q_e	Equilibrium dye concentration on nanocomposite (mg g^{-1})
q_m	Maximum adsorption capacity (mg g^{-1})
q_t	Amount of dye adsorbed at time t (mg g^{-1})
R	Universal gas constant ($8.314 \text{ J mol}^{-1} \text{ K}^{-1}$)
R^2	Correlation coefficient
ΔS^0	Entropy of reaction ($\text{J mol}^{-1} \text{ K}^{-1}$)
T	Temperature (K)
V	Volume of the solution (L)

M. K. Satapathy
Biotechnology Department, National Institute of Technology,
Durgapur, India

P. Banerjee
Department of Environment Science, University of Calcutta,
Kolkata, India

P. Das (✉)
Department of Chemical Engineering, Jadavpur University,
Kolkata, India
e-mail: papitasaha@gmail.com

Introduction

Progress in civilization and modernization, has led to high market demand rapidly and hence a rise in industrialization. But one recent global concern is the parallel development of various industries along with a drastic increase in industrial effluent discharge leading to environmental pollution as well as serious life-threatening problems for environment and normal flora of the affected region. Release of industrial effluent, often contaminated with toxic dyes, without proper and prior treatment into the environment is one of the major causes leading to a burden of health care issues in India and worldwide. One such usual toxic synthetic dye responsible for environmental pollution is crystal violet. For ages, it is being extensively used for biochemical analysis in medico-diagnostic laboratories, in food, pharmaceutical, plastic and textile industries. This dye is chemically classified as a synthetic basic dye group having a triphenylmethanolic structure. Due to its continuous discharge through the industrial effluents, it is now one of the most distressing issues amongst the environmental contaminants and pollution control measures (Ahmad 2009; Akar et al. 2009; Annadurai et al. 2002; Atmani et al. 2009; Namasivayam et al. 2001a, b; Saha et al. 2010). The toxic effects of crystal violet dye include cancer, methaemoglobinaemia, severe inflammatory responses in GI tract, eye irritation, cytogenetic toxicity (acts as mitotic poison), etc. Hence, the reclamation of water and prevention of environmental contamination is becoming a vital objective to attain using all possible measures. Presently, government legislations are forcing and promoting all the administrative bodies worldwide to determine appropriate solutions regarding industrial effluent treatment by focusing on innovating novel preventive and remedial measures and making them widespread. Current industrial and scientific research groups, academia, universities and reputed laboratories are active in researching and discovering novel, effective, environment-friendly, time-consumable and economic ways to curb environmental pollution and control-related issues (Ahmad 2009; Chowdhury and Saha 2010; Chakraborty et al. 2011; Chowdhury et al. 2013; Kumar and Ahmad 2011; Saeed et al. 2010; Senthilkumaar et al. 2006; Wang et al. 2008). Though the concepts of nanotechnology, bio-nanotechnology, bioprocessing, nano-adsorption and application of nanocomposite for dye removal have been in use for now, their applications and widespread acceptability are yet to mature and saturate. A step towards successful implementation of these above concepts is to implement them in a cost-effective and convenient method for dye removal from industrial effluent. Successful utilization of the aforesaid concepts lies in improvisation and utilization of conventional

methodologies. Soil is an example of one of the most important universal adsorbent due to its unique physico-chemical properties, structure, cost effectiveness as well as ease of availability. Hence, it can be modified for use as an effective adsorbent. In this study, a new soil composite is introduced for dye (crystal violet) removal from the industrial effluent with the aid of nanotechnology.

Silver nanoparticles (AgNPs) have been synthesized using biological and chemical process (El-Nour et al. 2010; Guzman et al. 2009; Natarajan et al. 2010; Prabhu and Poulouse 2012). More recently, plant-mediated synthesis (green synthesis) of silver nanoparticles have gained more importance (El-Nour et al. 2010; Guzman et al. 2009; Hah and Kao 2003; Mouxing et al. 2006; Prabhu and Poulouse 2012; Saha et al. 2011; Sulaiman et al. 2013; Xia et al. 2009) than those prepared chemically or microbially owing to the effectiveness (cost, time, ease of accessibility, etc.) of the process. Here, neem (*Azadirachta indica*) leaf extract is used as a cheap and chief source of reducing agent due to its wide availability throughout the year. These leaves are widely consumed in India for their antibacterial and medicinal properties. In the next step, soil (clay) is coated with these green synthesized AgNPs to form a novel green synthesized silver-nanocomposite to be used as an effective adsorbent for effective treatment of toxic dyes coming from industrial effluent. This nanocomposite is analysed to have excellent capability of toxic dye adsorption in laboratory scale. Optimisation of all experimental parameters has been determined with the help of batch experiments.

Materials and methodology

Collection of leaves and preparation of aqueous extract

Fresh healthy neem leaves (*A. indica*) collected from in and around Durgapur, were washed properly to remove the unwanted dust particles by thorough rinsing with double-distilled water and weighed afterwards. The leaves were then finely chopped followed by crushing 10 g of leaf in 100 mL double-distilled water and filtered to remove pigments and particulate matter. This filtrate was further used as a reducing agent.

Leaf extract-mediated synthesis of silver nanoparticles

Ninety-five mL of 1 mM silver nitrate solution was prepared in an Erlenmeyer flask of 250 mL capacity. 5 mL of aqueous leaf extract was then added dropwise to the silver nitrate solution. The colour change of the aqueous leaf extract, silver nitrate and the composite mixture were observed carefully in each and every step of the procedure.

Then the mixture was placed on the turntable of a microwave oven for complete bioreduction at a power level of 300 W for 5 min. As the colour of the mixture changed from faint light green to light yellowish-brown to reddish brown to colloidal brown, the absorption maxima of the solution was measured by a spectrophotometer at an interval of every 30 min, throughout the reaction. After irradiation, the dilute colloidal solution was cooled to room temperature and kept aside for 24 h to obtain complete bioreduction and saturation. Then the colloidal mixture was stored properly for future use. In each and every step during the whole experiment, control samples were also analysed.

Analysis of silver nanoparticles

The bioreduction and silver nanoparticle formation was confirmed by monitoring the periodic samples collected from the colloidal mixture solution by UV–visible spectrophotometer at around 457 nm. The scanning observation were carefully monitored and recorded.

Preparation of biomimetic silver-nanocomposite

Soil collected for preparation of nanocomposite was weighed and churned into fine particles, sieved and slowly added to the nanoparticle-containing solution and mixed properly for silver nanocoating and composite adsorbent preparation. The composite mixture solution was kept overnight in a shaker incubator for the reaction to occur in between the silver nanoparticle and the clayey soil. After 24 h incubation at a particular agitation speed, the solution was kept for settling of the nanocomposite. The supernatant was discarded and the composite mixture was dried. The dried nanocomposite was again finely churned and sieved to get the nano-sized composite soil particle and used as effective adsorbent for dye removal.

Preparation of adsorbate solution

Crystal violet (CV) was purchased (Merck, Germany) (MF, $C_{25}H_{30}N_3Cl$; MW, 408; λ_{max} , 580 nm) and was used for further study. Stock solution of dye was prepared by dissolving accurate quantity of the solid dye in double-distilled water. Different concentrations of dye were prepared by diluting the stock solution. The initial solution pH was adjusted using 0.1 N HCl and 0.1 N NaOH solutions (Chakraborty et al. 2011; Chowdhury et al. 2013).

Characterization of the nanocomposite

The prepared silver nanoparticle and the soil composite adsorbent were characterized by SEM, FTIR, and XRD.

Scanning electron microscopy analysis

Scanning electron microscopy revealed the surface morphology of the nanocomposite. The study was conducted using a scanning electron microscope (Model Hitachi S-3000N) at an electron acceleration voltage of 20 kV. The samples were coated with a thin layer of gold using a sputter coater to make them conductive and then used for scanning.

Fourier transform infrared spectroscopy analysis

Functional groups present on the nanoparticle can be identified by Fourier transform infrared (FTIR) spectroscopy as each group has a unique energy absorption band. Therefore, FTIR spectra were recorded using FTIR spectrophotometer (Perkin-Elmer Spectrum BX-II Model) in the wavenumber range $4,000\text{--}500\text{ cm}^{-1}$ at 4 cm^{-1} spectral resolution.

XRD analysis

X-ray diffraction analysis of the nanocomposite adsorbent was carried out using Miniflex X-ray diffractometer equipment with a CuK_{α} radiation source.

Batch experiments

Batch experiments were carried out in 250-mL Erlenmeyer flasks with 100 mL of dye solution. A weighed amount (1 g) of nanocomposite was added to the dye solution. The flasks were agitated at a constant speed of 180 rpm in an incubator shaker (Model Innova 42, New Brunswick Scientific, Canada) at $308 \pm 1\text{ K}$. The influence of pH (2.0–10.0), initial dye concentration ($10\text{--}200\text{ mg L}^{-1}$), nanocomposite dosage ($0.5\text{--}10\text{ g/L}$) and temperature (298, 303, 310, 313, 318 K) were evaluated. Samples were collected at predetermined time intervals for analysing the residual dye concentration in the solution. The residual amount of dye in each flask was investigated using UV/VIS spectrophotometer (Model Hitachi-2800, Japan). The amount of dye adsorbed per unit of nanocomposite was determined according to a mass balance using Eq. 1:

$$q_e = \frac{(C_i - C_e) V}{m} \quad (1)$$

where C_i is the initial dye concentration (mg L^{-1}), C_e is the equilibrium dye concentration in solution (mg L^{-1}), V is the volume of the solution (L), and m is the mass of the nanocomposite in g. The percent removal (%) of dye was calculated using the following equation:

$$\text{Removal (\%)} = \frac{C_i - C_e}{C_i} \times 100 \quad (2)$$

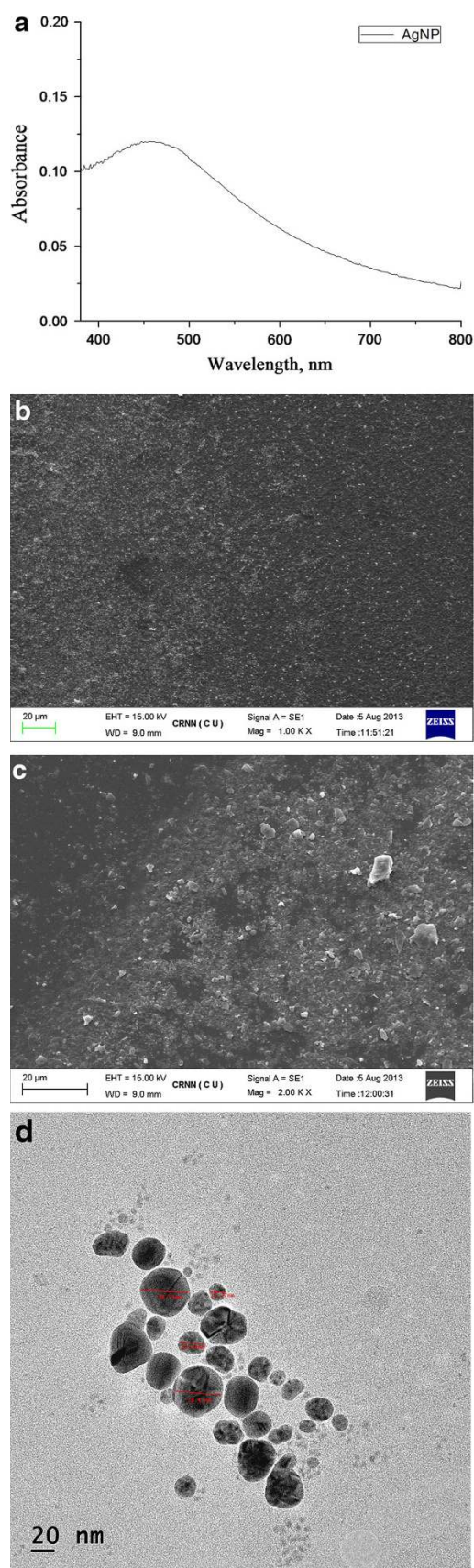


Fig. 1 **a** Absorbance peak of Ag-nanoparticle after 24 h. **b** SEM analysis of synthesized Ag-nanoparticle. **c** SEM analysis of Ag-nanocomposite materials. **d** TEM analysis of the synthesized Ag-nanoparticle

In order to ensure the reproducibility of the results, all the adsorption experiments were performed in triplicate, and the mean values were used in data analysis. The error obtained was found to be within ± 3.0 %. Microsoft Excel 2007 program was employed for data processing.

Results and discussion

The formation of AgNPs in the solution of 1 mM silver nitrate and aqueous extract of the *A. indica* leaf sample was confirmed by change in the colour to reddish brown after incubation with silver nitrate, while the controls retained the original colour of the extract.

The synthesis of Ag nanoparticles in aqueous extract was monitored by collecting the samples of the reaction mixture at regular intervals and monitored using UV–VIS spectroscopy. The AgNPs exhibits yellowish-brown colour in water and the reason of this colour may be due to the excitation of surface plasmon vibrations. Figure 1a shows the UV–Vis spectra recorded from the aqueous silver nitrate-*A. indica* leaf after 24 h. The highest absorbance peak was observed at around 457 nm after different time intervals.

Figure 1b represents synthesized AgNPs and Fig. 1c represents the AgNPs coated on the surface of soil particles. From TEM analysis (Fig. 1d), the distribution of different-sized Ag-nanoparticle was observed. It was observed that most of the AgNP was in the range of 38–42 nm and average size of the nanoparticle was 38.8 nm.

FTIR spectral analysis (figure not shown) showed array of absorbance bands in $500\text{--}4,000\text{ cm}^{-1}$. The spectral bands were prominent at 721, 1,637.27, 2,364.3, 3,334.1 and $3,745.08\text{ cm}^{-1}$ which were interpreted for the identification of the functional moieties in the aqueous AgNPs. These bands were mainly due to the presence of chloride, alkene, carboxyl and hydrogen bond present in the sample. XRD analysis of Ag-nanocomposite (figure not shown) demonstrated that major components present in nanocomposite were Ag, quartz, illite, feldspar, kaolinite, montmorillonite, and calcite due to the presence of soil in the composite.

The collected soil sample had a pH of 7.5, moisture content of 26 %, with cation exchange capacity of 31.82 (mequiv/100 g dry soil) bearing a surface area of $61\text{ m}^2/\text{g}$, clay 27 %, silt 68 % and sand 5 %.

Effect of operating parameters

Five g/L soil and 5 g/L Ag-nanocomposite was used as adsorbent for treatment of 100 mL of 20 mg/L of solution separately. It was observed (Fig. 2) that using Ag-nanocomposite, the adsorption capacity and % removal of crystal violet dye increased by 12-fold after 1 h of incubation period.

Effect of Ag-nanocomposite dose

Since adsorption capacity is known to influence the adsorption process, adsorbent dose is an important parameter for a particular initial concentration of the adsorbate under the experimental operating conditions. The pH of the solution was measured and controlled throughout the experiment. The pH of the solution was measured for

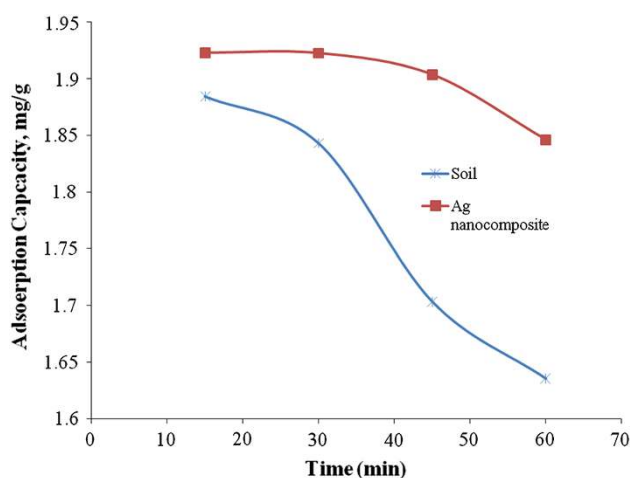


Fig. 2 Comparative analysis of adsorption capacity of dye using soil and Ag-nanocomposite using 1 g of adsorbent, 20 mg/L concentration of dye, 180 rpm agitation speed at 313 K temperature

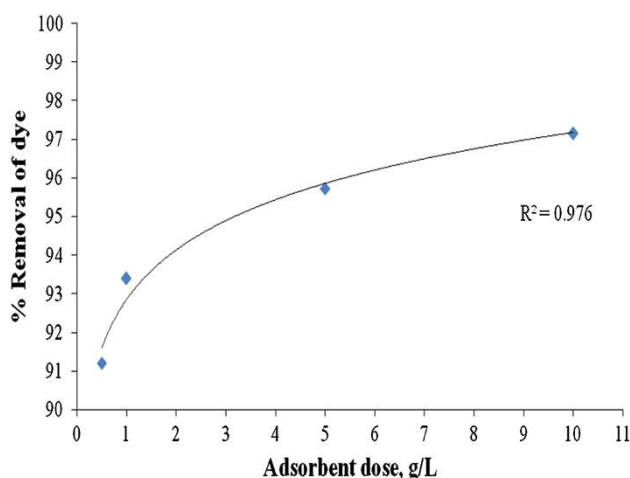


Fig. 3 Effect of Ag-nanocomposite dose on the removal of CV dye on 100 mL of 20 mg/L of solution, 180 rpm at 313 K

all the experiments before and after adsorption experiments. The experiment was performed until equilibrium was attained between the solution and the nanocomposite materials. From Fig. 3, it was observed that the adsorption efficiency increased from 91.2 to 97.2 % as the adsorbent dose increased from 0.5 to 10 g/L. The increase in the percentage of dye removal with adsorbent dosage may be attributed to an increase in the nanocomposite surface area available for adsorption, as already reported (Ahmad 2009). These observations are also in agreement with those previously reported by other researchers for the sorption of dyes by different adsorbents (Ahmad 2009; Wang et al. 2008).

Effect of initial dye concentration

The adsorption process is influenced by the initial concentration of the adsorbate concentration. Therefore, the effect of different initial dye concentrations on adsorption onto nanocomposite was also investigated. The amount of dye adsorbed per unit mass of the nanocomposite increased with increase in the initial dye concentration. As observed in Fig. 4, the adsorption capacity at equilibrium increased from 1.92 to 35.97 mg g⁻¹ with increase in initial dye concentration from 10 to 200 mg L⁻¹. This behaviour may be a result of the increase in the driving force from the concentration gradient. Additionally, if the concentration of CV in solution is higher, the active sites of the adsorbent may have been surrounded by many more CV ions leading to the occurrence of a more efficient adsorption phenomenon. Hence, in accordance with the results obtained by Chowdhury et al. (2013) adsorption capacity increased with the increase of initial dye concentrations.

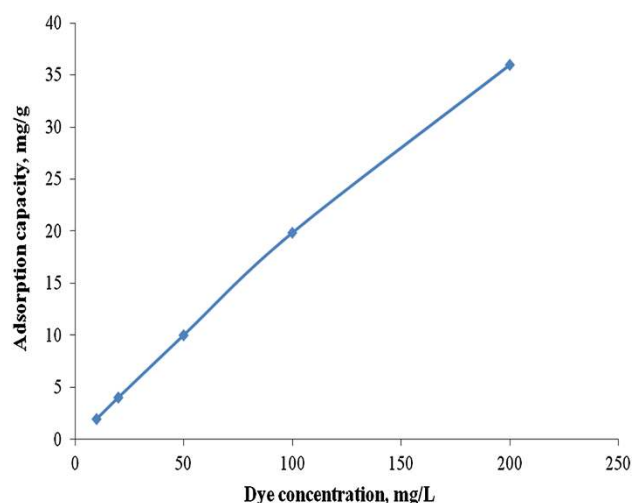


Fig. 4 Effect of initial dye concentration on removal of CV dye using Ag-nanocomposite on 100 mL of 20 mg/L of dye solution at 180 rpm at 313 K

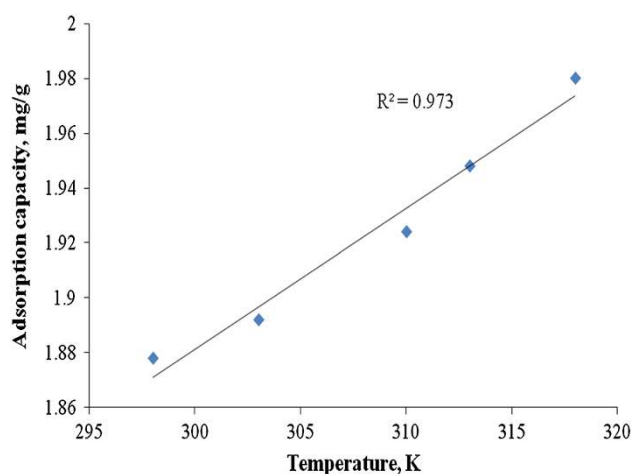


Fig. 5 Effect of temperature on removal of CV dye using Ag-nanocomposite on 100 mL of 20 mg/L of dye solution at 180 rpm

Effect of temperature

Since temperature is an important design parameter influencing adsorption capacity, batch experiments were performed at different temperature ranges (from 298 to 318 K). Data obtained from the experiments are presented in Fig. 5. It was observed that all other conditions remaining unaltered, the percentage of dye removal increased with rise in temperature from 298 to 318 K. The increase in percentage removal of dye with increase in temperature may be explained by the increased affinity of binding sites for dye molecules at higher temperature. An increase in temperature also resulted in an increase in mobility of the dye molecules and a decrease in the retarding forces acting on the molecules; thus, enhancing the dye-binding capacity of the adsorbent. The observed trend in increased dye-removal capacity with increase in temperature suggested that the adsorption of dye by the nanocomposite was kinetically controlled by an endothermic process. A similar trend was reported for adsorption of CV onto treated ginger waste by Kumar and Ahmad (2011).

Adsorption isotherms

Different isotherm models were employed to examine the relationship between the amount of adsorbate (q_e) and its concentration in the aqueous phase (C_e) at equilibrium. In the present investigation, the results of adsorption studies of dye at various temperatures onto a nanocomposite were fitted to models of Freundlich, Langmuir (Chowdhury et al. 2011, 2013; Freundlich 1906; Langmuir 1916):

$$\text{Langmuir: } \frac{C_e}{q_e} = \frac{C_e}{q_m} + \frac{1}{K_L q_m} \quad (3)$$

Table 1 Adsorption isotherm constants for sorption of CV onto nanocomposite at different temperatures

Temp	Langmuir isotherm parameters			Freundlich isotherm parameters		
	q_m (mg g ⁻¹)	K_L (L mg ⁻¹)	R^2	K_F (mg g ⁻¹) (L mg ⁻¹) ^{1/n}	n	R^2
298	1.858	31.25	0.999	1.898	31.25	0.966
303	1.891	200.2	1.000	1.917	50.00	0.997
310	1.918	260	0.999	1.923	66.66	0.962
313	1.919	260.55	1.000	1.925	71.428	0.936
318	1.919	261.09	0.999	1.926	71.66	0.944

$$\text{Freundlich: } \log q_e = \log K_F + \left(\frac{1}{n}\right) \log C_e \quad (4)$$

The parameters and correlation coefficients obtained from the plots of Langmuir (C_e/q_e versus C_e), Freundlich ($\log q_e$ versus $\log C_e$) (figures not shown) are listed in Table 1.

From the experimental results (Table 1), it was observed that sorption of CV onto nanocomposite followed the Langmuir model. The excellent fit of the Langmuir isotherm to the experimental data at all temperatures studied confirmed that the adsorption is monolayer; sorption of each molecule had equal activation energy and that sorbate–sorbate interaction was negligible. Increase in both q_m and K_L values with increase in temperature specified the adsorption process to be endothermic nature. The monolayer adsorption capacity of Ag-nanocomposite for CV as obtained from the Langmuir isotherm at 313 K was found to be 1.919 mg g⁻¹. The estimated coefficients of the Freundlich model (K_F and n) for CV adsorption onto Ag-nanocomposite at different temperatures are listed in Table 1. The K_F value represented the degree of adsorption. The K_F values showed that the adsorption rate increased with the rise of temperature. $n > 1$ illustrated that adsorbate was favourably adsorbed on an adsorbent, and the higher n value suggested a stronger adsorption intensity. For the present study, the value of n was higher than unity, indicating that CV ions were favourably adsorbed on nanocomposite under all the temperatures studied.

Adsorption kinetics

The study of adsorption kinetics described the adsorbate uptake rate and evidently, this rate controlled the residence time of adsorbate at the solid–liquid interface. In order to analyse the adsorption kinetics of CV onto nanocomposite, the Lagergren's pseudo-first-order and Ho–McKay's

pseudo-second-order models (Ho and McKay 1999) were applied to the experimental data.

$$\text{Pseudo-first-order: } \log(q_e - q_t) = \log q_e - \frac{k_1}{2.303} t \quad (7)$$

$$\text{Pseudo-second-order: } \frac{t}{q_t} = \frac{1}{k_2 q_e^2} + \frac{1}{q_e} t. \quad (8)$$

The values of pseudo-first-order rate constants, k_1 and q_e were calculated from slopes and intercepts of the plots of $\log(q_e - q_t)$ versus t (figure not shown). The R^2 values suggested that adsorption of CV onto nanocomposite did not follow pseudo-first-order kinetics. In addition, the theoretical and experimental equilibrium adsorption capacities, q_e obtained from these plots varied widely, confirming that the pseudo-first-order model was not appropriate for describing the adsorption kinetics of CV onto nanocomposite. On the contrary, the kinetic data showed excellent fit to the pseudo-second-order equation at all temperatures studied. K_2 from second-order kinetic study was evaluated as $31.25 \text{ g mg}^{-1} \text{ min}^{-1}$ (at 310 K) and R^2 was 0.999. It can thus be concluded that the reaction proceeded following a pseudo-second-order mechanism rather than a pseudo-first-order mechanism.

During batch mode of operation, there was a possibility of intra-particle pore diffusion of adsorbate ions, which could have been the rate-limiting step. Therefore, the possibility of intra-particle diffusion resistance affecting the adsorption process was explored by using the intra-particle diffusion model as (Ahmad 2009; Chowdhury et al. 2013; Gong et al. 2008):

$$q_t = k_i t^{0.5} + I. \quad (9)$$

According to Eq. 9, a plot of q_t versus $t^{0.5}$ should be a straight line (figure not shown) with a slope k_i and intercept I when the adsorption mechanism follows the intra-particle diffusion process. However, if the data exhibit multi-linear plots, then the process is governed by two or more steps.

The adsorption of CV on nanocomposite at different temperatures was three distinct regions (figure not shown). The initial curved region attributes to the external surface adsorption in which the adsorbate diffuses through the solution to the external surface of the nanocomposite. The second stage denotes the gradual uptake reflecting intra-particle diffusion as the rate-limiting step. The final plateau region refers to the gradual adsorption stage and the final equilibrium stage, in which the intra-particle diffusion starts to slow down and level out. The present finding implies that although intra-particle diffusion is involved in the adsorption process, it is not the sole rate-controlling step and that some other mechanisms also play an important role. Similar results were also previously reported for adsorption of basic dyes by various low-cost adsorbents.

Adsorption thermodynamics

Activation energy

Activation energy E_a for adsorption of CV onto nanocomposite was determined using the Arrhenius equation:

$$\ln k = \ln A - \frac{E_a}{RT}. \quad (12)$$

Plotting $\ln k$ against the reciprocal temperature (Fig. 6) gives a reasonably straight line. The value of E_a can be determined from the slope of the linear plot of $\ln k$ versus $1/T$.

From experimental results, it was observed that activation energy, E_a for the adsorption of CV onto nanocomposite was $65.780 \text{ kJ mol}^{-1}$. E_a for physisorption is usually less than 40 kJ mol^{-1} , as the forces involved in this case is physical sorption, and so they are weak. On the other hand, higher values represent chemical reaction process and so chemisorption is specific in nature and involves forces

Fig. 6 Arrhenius equation plot for adsorption of CV dye onto Ag-nanocomposite

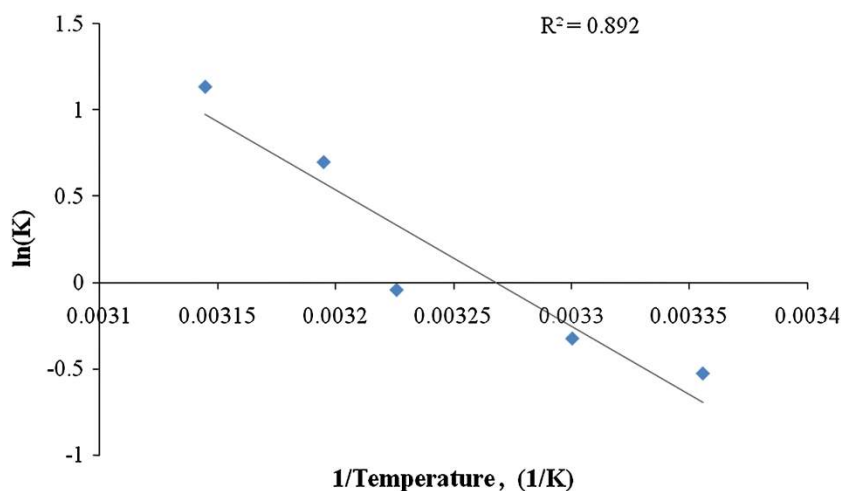


Table 2 Thermodynamic parameters for adsorption of CV onto nanocomposite

ΔG^0 (kJ mol ⁻¹)					ΔH^0 (kJ mol ⁻¹)	ΔS^0 (J mol ⁻¹ K ⁻¹)
298 K	303 K	308 K	311 K	318 K		
-6.81	-7.215	-8.391	-8.565	-14.499	91.053	324

much stronger than those involved in physisorption. The calculated E_a value was higher than 40 kJ mol⁻¹ suggesting that the adsorption process of CV on nanocomposite followed chemisorption.

Thermodynamic parameters

Thermodynamic considerations of an adsorption process are necessary to conclude whether the process is spontaneous or not. Therefore, Gibbs free energy change (ΔG^0), enthalpy (ΔH^0) and entropy (ΔS^0) were calculated to evaluate the thermodynamic feasibility of the process and to confirm the nature of the adsorption process. Thermodynamic parameters were calculated by applying the equations:

$$\Delta G^0 = -RT \ln K_C \quad (13)$$

$$K_C = \frac{C_a}{C_e} \quad (14)$$

$$\Delta G^0 = \Delta H^0 - T\Delta S^0 \quad (15)$$

The plot of ΔG^0 versus T (figure not shown) gave a straight line with the slope and intercept giving the values of ΔH^0 and ΔS^0 , respectively. Table 2 showed the value of the thermodynamic parameters of CV adsorption on Ag-nanocomposite. The negative value of ΔG^0 at all temperatures confirmed that the process was spontaneous. Positive value of ΔH^0 implied that the adsorption process was endothermic. The positive value of ΔS^0 indicated the affinity of the adsorbent for the dye removal and an increased randomness at the solid–solution interface during adsorption.

Conclusion

The following conclusions are made based on the results of present study:

The % dye removal was 97.2 % and endothermic nature.

The Langmuir isotherm model provided best fit to the experimental equilibrium data indicating monolayer sorption on a homogenous surface.

The activation energy of the adsorption process (E_a) was found to be 65.78 J mol⁻¹ indicating chemisorption nature and negative value of Gibb's free energy (ΔG^0) indicating the spontaneity and feasibility of the adsorption process.

Overall, the results suggest that this environmentally sustainable, economically convenient and efficient adsorbent may be considered useful for the removal of CV from effluent solution.

Open Access This article is distributed under the terms of the Creative Commons Attribution License which permits any use, distribution, and reproduction in any medium, provided the original author(s) and the source are credited.

References

- Ahmad R (2009) Studies on adsorption of crystal violet dye from aqueous solution onto coniferous pinus bark powder (CPBP). *J Hazard Mater* 171:767–773
- Akar ST, Özcan AS, Akar T, Özcan A, Kaynak Z (2009) Biosorption of a reactive textile dye from aqueous solutions utilizing an agro-waste. *Desalination* 249:757–761
- Annadurai G, Juang R-S, Lee D-J (2002) Use of cellulose-based wastes for adsorption of dyes from aqueous solutions. *J Hazard Mater* 92:263–274
- Atmani F, Bensmaili A, Mezenner NY (2009) Synthetic textile effluent removal by skin almond waste. *J Env Sci Technol* 2:153–169
- Chakraborty S, Chowdhury S, Saha PD (2011) Adsorption of crystal violet from aqueous solution onto NaOH-modified rice husk. *Carbohydr Polym* 84:1533–1541
- Chowdhury S, Saha P (2010) Sea shell powder as a new adsorbent to remove Basic Green 4 (Malachite Green) from aqueous solutions: equilibrium, kinetic and thermodynamic studies. *Chem Eng J* 164:168–177
- Chowdhury S, Mishra R, Saha P, Kushwaha P (2011) Adsorption thermodynamics, kinetics and isosteric heat of adsorption of malachite green onto chemically modified rice husk. *Desalination* 265:159–168
- Chowdhury S, Chakraborty S, Saha PD (2013) Response surface optimization of a dynamic dye adsorption process: a case study of crystal violet adsorption onto NaOH-modified rice husk. *Env Sci Polln Res* 20(3):1698–1705. doi:10.1007/s11356-012-
- El-Nour KMM, Eftaiha A, Al-Warthan A, Ammar RAA (2010) Synthesis and applications of silver nanoparticles. *Arab J Chem* 3:135–140
- Freundlich HMF (1906) Over the adsorption in solution. *J Phys Chem* 57:385–471
- Gong R, Zhu S, Zhang D, Chen J, Ni S, Guan R (2008) Adsorption behavior of cationic dyes on citric acid esterifying wheat straw: kinetic and thermodynamic profile. *Desalination* 230:220–228
- Guzman MG, Dille J, Godet S (2009) Synthesis of silver nanoparticles by chemical reduction method and their antibacterial activity. *Int J Chem Biol Eng* 2(3):104–111
- Hah JH, Kao SM (2003) Preparation of silver nanoparticles through alcohol reduction with organoalkoxysilanes. *J Sol-Gel Sci Technol* 26:467–471
- Ho YS, McKay G (1999) Pseudo-second-order model for sorption processes. *Proc Biochem* 34:451–465

- Kumar R, Ahmad R (2011) Biosorption of hazardous crystal violet dye from aqueous solution onto treated ginger waste (TGW). *Desalination* 265:112–118
- Langmuir I (1916) The constitution and fundamental properties of solids and liquids. *J Am Chem Soc* 38:2221–2295
- Mouxing F, Qingbiao L, Daohua S, Yinghua L, Ning H, Xu D, Huxan W, Jiale H (2006) Rapid preparation process of silver nanoparticles by bioreduction and their characterizations. *Chin J Chem Eng* 14(1):114–117
- Namasivayam C, Dinesh Kumar M, Selvi K, Begum RA, Vanathi T, Yamuna RT (2001a) ‘Waste’ coir pith—a potential biomass for the treatment of dyeing wastewaters. *Biomass Bioenergy* 6:477–483
- Namasivayam C, Radhika R, Suba S (2001b) Uptake of dyes by a promising locally available agricultural solid waste: coir pith. *Waste Manag* 21:381–387
- Natarajan K, Selvary S, Murty RV (2010) Microbial production of silver nanoparticles. *Dig J Nanomater Bios* 5:135–140
- Prabhu S, Poulouse EK (2012) Silver nanoparticles: mechanism of antimicrobial action, synthesis, medical applications, and toxicity effects. *Int Nano Lett* 2:32–42
- Saeed A, Sharif M, Iqbal M (2010) Application potential of grapefruit peel as dye sorbent: kinetics, equilibrium and mechanism of crystal violet adsorption. *J Hazard Mater* 179:564–572
- Saha P, Chowdhury S, Gupta S, Kumar I (2010) Insight into adsorption equilibrium, kinetics and thermodynamics of malachite green onto clayey soil of Indian origin. *Chem Eng J* 165:874–882
- Saha S, Chattopadhyay D, Acharya K (2011) Preparation of silver nanoparticles by bio-reduction using *Nigrospora Oryzae* culture filtrate and its antimicrobial activity. *Dig J Nanomater Bios* 6:1519–1528
- Senthilkumaar S, Kalaamani P, Subburaam CV (2006) Liquid phase adsorption of crystal violet onto activated carbons derived from male flowers of coconut. *J Hazard Mater* 136:800–808
- Sulaiman GM, Mohammad WH, Marzay TR, Al-Amiery AAA, Kadhum AAH, Mohammad AB (2013) Green synthesis, antimicrobial and cytotoxic effects of silver nanoparticles using *Eucalyptus chapmaniana* leaves extract. *Asian Pac J Trop Biomed* 3(1):58–63
- Wang XS, Liu X, Wen L, Zhou Y, Li Z (2008) Comparison of basic dye crystal violet from aqueous solution by low-cost biosorbents. *Sep Sci Technol* 43:3712–3731
- Xia Y, Xiong YJ, Lim B, Skrabalak SE (2009) Shape-controlled synthesis of metal nanocrystals: simple chemistry meets complex physics? *Angew Chem Int Ed* 48(1):60–103